

# Controlling Autoreclosing on Overhead Lines With Underground Cable Sections Using Traveling-Wave Fault Location Based on Measurements From Line Terminals Only

B. Kasztenny, A. Guzmán, M. V. Mynam, and T. Joshi  
*Schweitzer Engineering Laboratories, Inc.*

Presented at the  
14th International Conference on Developments in Power System Protection  
Belfast, United Kingdom  
March 12–15, 2018

# Controlling autoreclosing on overhead lines with underground cable sections using traveling-wave fault location based on measurements from line terminals only

B. Kasztenny\*, A. Guzmán\*, M. V. Mynam\*, T. Joshi\*

\*Schweitzer Engineering Laboratories, Inc., 2350 NE Hopkins Court, Pullman, WA 99163 USA  
bogdan\_kasztenny@selinc.com

**Keywords:** traveling waves, fault locating, cable lines, autoreclosing.

## Abstract

The paper explains principles of fault locating based on traveling waves measured only at line terminals for hybrid lines comprising overhead and cable sections. The paper introduces an adaptive autoreclosing control logic to allow or cancel reclosing based on the location of the fault. The paper includes examples that explain and illustrate these principles.

## 1 Introduction

Historically, fault location information has been provided to a line maintenance crew just in time for them to inspect and repair a line after a permanent fault. Today, with impedance-based fault locating widely available in microprocessor-based protective relays integrated with SCADA, system operators have access to fault location information within seconds.

The next step in the practice of fault locating embedded in protective relays is to provide the fault type and accurate fault location information within milliseconds, in order to facilitate control functions such as adaptive control of autoreclosing.

Today, impedance-based fault locators, especially the single-ended ones, do not guarantee enough accuracy under all fault conditions to support controlling the reclosing logic based on the fault location. Also, today's relays do not typically calculate fault location quickly enough to use it for adaptive control of autoreclosing.

This paper reviews technical, safety, and economical merits of adaptive autoreclosing based on fault location, and it presents a method for accurate fault locating using traveling waves (TWs) from both terminals of the line to facilitate such location-dependent "surgical autoreclosing" [1]. The paper illustrates the new principles with simulations and test results from a line relay that provides the first-ever adaptive autoreclosing logic controlled by fault location.

## 2 Applications and benefits of autoreclosing controlled by fault location

### 2.1 Hybrid lines with overhead line sections and underground cable sections

Hybrid lines comprising overhead line sections and underground cable sections are becoming more common, especially in urban areas. The underground cable sections are typically more expensive and are only used to cross densely populated areas, airports, highways, or terrain where obtaining an above-the-ground right-of-way is difficult for a variety of reasons, including environmental and aesthetic constraints. A hybrid line can have more than one underground cable section.

Many faults on overhead lines are temporary faults, allowing for a high rate of successful autoreclosing [2]. In contrast, all faults on underground cables are permanent faults. Precursors to faults (incipient faults) are transient in nature, but once the solid cable insulation is damaged, it will not restore itself. Autoreclosing for faults on cables is counterproductive; it further damages the cable causing longer and more expensive repair.

Ideally, you would prefer to allow autoreclosing on overhead line sections and to block autoreclosing on underground cable sections of a hybrid line. In single-pole tripping applications, a single-pole trip for a fault on a cable section should be converted into a three-pole trip, and the autoreclosing scheme should not reclose for that fault.

Today, there are no economical solutions to facilitate this application. Reference [3] proposes installing current transformers (CTs) at each transition between a cable and an overhead line section and obtaining current measurement via a fiber-optic connection to one of the line terminals. Using the current measurement at each transition point, the logic implements a differential zone for each cable section and sends a block command to the autoreclosing device if the fault is in one of the cable sections (in one of the differential zones). To avoid electronics and having to bring auxiliary control power to the CTs located along the line, solution [3] uses a piezoelectric element to convert the current signal into a mechanical displacement signal. Further, it uses a Bragg-effect fiber-optic filter to sense the mechanical displacement remotely with the laser source and the associated sensing electronics located at the main line terminal. This solution has

the drawback of requiring CTs at each transition point and fiber-optic cables from each of these CTs to the main line terminal where the autoreclosing device is located.

Another solution to the adaptive control of autoreclosing of hybrid lines is to use fault location information obtained using measurements only at the line terminals. However, impedance-based fault-locating methods do not have adequate accuracy for this application because of a number of factors (see Section 3).

This paper shows that the double-ended TW-based fault-locating method with correction for line nonhomogeneity provides an accurate fault location for adaptive autoreclosing on hybrid lines.

## 2.2 Other applications of adaptive autoreclosing

### 2.2.1 Lines terminating at large generating stations

Reclosing for a permanent fault near a generating station has adverse effects on generators and turbines [2]. Large transient torque created when closing on a high-current fault stresses the generator shaft, turbine shaft, their bearings, and other mechanical components of the unit. The best reclosing practice for these lines is to test the line from the remote line terminal (the terminal away from the generating station) and then reclose the circuit breaker at the generator terminal with synchronism-check supervision [2]. Some lines, however, have generating stations close to both terminals. Inhibiting autoreclosing for high-current close-in faults but allowing reclosing for lower-current remote faults reduces the mechanical stress on the generator and the turbine.

### 2.2.2 Lines with public safety concerns

Reclosing onto a permanent fault creates a second high-energy event at the fault location, in addition to the initial fault. There are several situations when it may be beneficial to avoid reclosing. They include:

- Highly populated areas, such as subtransmission lines sharing the right-of-way with roads or even residential streets. Not reclosing for fault locations where humans are likely to be present improves safety.
- Airports, especially regional airports receiving small airplanes operated by amateur pilots. Not reclosing for fault locations where a small airplane may have inadvertently flown into the line is beneficial.
- Fire-prone terrain such as forests or bush areas, especially in very dry climates or seasons. Not reclosing for faults on these fire-prone stretches of the line reduces the potential of starting large and expensive wildfires.

### 2.2.3 Lines with sections having a low success rate of autoreclosing

Some lines may experience a very low autoreclosing success rate for faults on certain sections depending on construction or surroundings of these sections. Location-dependent autoreclosing offers an option to block reclosing for these low-success-rate sections, while allowing reclosing for faults elsewhere on the line.

## 3 Fault locating on hybrid lines with overhead line sections and underground cable sections

### 3.1 Limitations of impedance-based methods

Impedance-based fault-locating methods using the total line impedance value of the hybrid line face the following challenges [4]:

- The positive-sequence impedance per mile is very different for the overhead sections and cable sections.
- The  $Z_0/Z_1$  ratio is very different for the overhead sections and cable sections.
- The zero-sequence impedance for cable sections can be a nonlinear function of the fault current, is uncertain, and it depends on the grounding and shielding methods and other conductive paths in the vicinity [4].

In addition, the following common factors affect the accuracy of impedance-based methods in general:

- Ratio errors in CTs and voltage transformers (VTs).
- Phasor measurement errors in the fault-locating device.
- Uncertainty in line impedance data.
- Impact of fault resistance and changes in fault resistance.
- Impact of the line charging current.

As a result of the general accuracy-limiting factors and accuracy-limiting factors specific to cables and hybrid lines, the expected fault-locating accuracy of impedance-based methods in cables or hybrid lines can be on the order of 10 percent or worse, and it is insufficient to support the adaptive autoreclosing application.

### 3.2 Double-ended TW-based fault-locating principle

Fig. 1 shows a Bewley diagram for a fault at location F on a line of length LL. The fault is M (km or mi) away from the local terminal (S) and  $LL - M$  (km or mi) away from the remote terminal (R). The TW propagation velocity (PV) for the line is the ratio of the total line length (LL) and the TW line propagation time (TWLPT) settings of the fault locator:

$$PV = \frac{LL}{TWLPT} \quad (1)$$

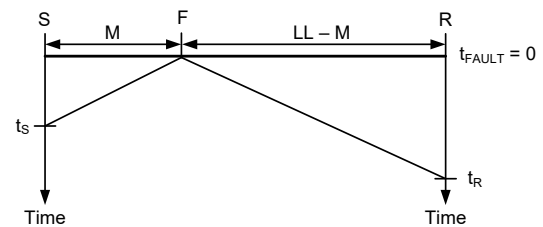


Fig. 1. Bewley diagram explaining double-ended TW-based fault locating.

The first current TW arrives at Terminal S at:

$$t_s = \frac{M}{PV} \quad (2)$$

The first current TW arrives at Terminal R at:

$$t_R = \frac{LL - M}{PV} \quad (3)$$

Solving (2) and (3) for the fault location,  $M$ , and factoring in (1) for the propagation velocity, we obtain the following fault-locating equation:

$$M = \frac{LL}{2} \cdot \left( 1 + \frac{t_S - t_R}{TWLPT} \right) \quad (4)$$

The fault-locating method (4) measures current TWs by using a differentiator-smoother filter [5]. A practical implementation [6] of this method applies the differentiator-smoother filter to current samples taken every microsecond. The method further incorporates a time-stamping algorithm that uses interpolation to find the time of the peak for the output of the differentiator-smoother filter. This interpolation provides a time-stamping accuracy of approximately  $0.1 \mu\text{s}$ , i.e., about ten times better than the sampling interval.

The double-ended TW-based fault-locating method (4) is simple, yet very accurate. It requires identifying and time-stamping only the very first TWs at both line terminals. Not having to isolate and identify the origin of any subsequent TWs is a great advantage of this fault-locating method [5] compared with the single-ended method. Because (4) is a double-ended method, it requires the TW-based fault-locating devices at both line terminals to be synchronized so that the TW arrival times at both line terminals are captured with the same time reference. The synchronization is typically achieved using satellite-synchronized clocks or using a direct point-to-point fiber-optic channel between the devices [1].

The double-ended TW-based fault-locating method (4) has a field-proven track record with reported accuracy within one tower span (300 m or 1000 ft) on average [5]. When tested under ideal conditions, the double-ended TW-based fault-locating method (4) implemented on a hardware platform [6] yields a 90th percentile error considerably below 20 m (66 ft) and a median error less than 10 m (33 ft).

### 3.3 Double-ended TW-based fault locating for hybrid lines

Consider the hybrid line depicted in Fig. 2, comprising two overhead line sections, 1 and 3, and one underground cable section, 2. The overhead section lengths are  $LL_1$  and  $LL_3$  and the cable section length is  $LL_2$ . The TW line propagation times for the overhead line sections are  $TWLPT_1$  and  $TWLPT_3$  and the TW line propagation time for the cable section is  $TWLPT_2$ .

Expect different propagation velocities for the overhead and cable sections as follows:

$$\frac{LL_1}{TWLPT_1} \cong \frac{LL_3}{TWLPT_3} \gg \frac{LL_2}{TWLPT_2} \quad (5)$$

For example, the propagation velocity for the overhead line sections can be approximately 98 percent of the speed of light in free space, while the propagation velocity for the cable

section can be as low as 50 percent of the speed of light in free space.

The line of Fig. 2a can be conveniently depicted as a piecewise linear characteristic representing the relationship between the distance-to-fault and the TW line propagation time to the fault location (Fig. 2b).

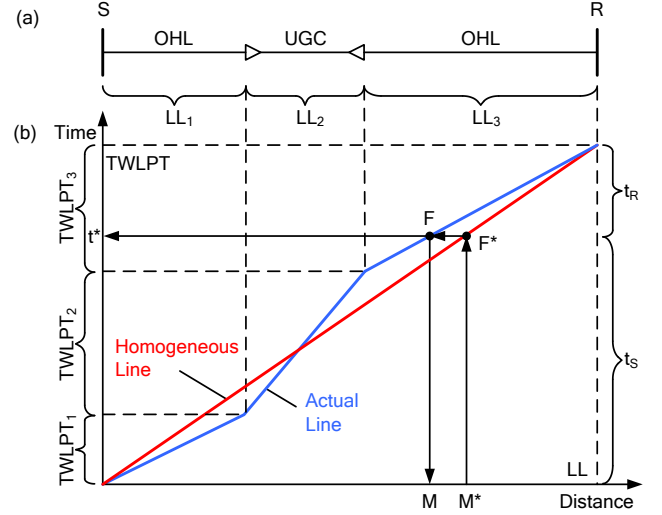


Fig. 2. Sample hybrid line with two overhead sections and one cable section (a) and its distance-propagation time characteristic (b).

Let us denote the total line length as  $LL$ :

$$LL = LL_1 + LL_2 + LL_3 \quad (6)$$

and the total TW line propagation time as  $TWLPT$ :

$$TWLPT = TWLPT_1 + TWLPT_2 + TWLPT_3 \quad (7)$$

For any fault location ( $F$ ), if one line terminal measures the TW arrival time as  $t_s$ , the other terminal measures the TW arrival time as  $t_r = TWLPT - t_s$  (see Fig. 2b).

Assume we use the fault-locating method (4) neglecting the line nonhomogeneity, i.e., we use (4) with the total line length (6) and the total TW line propagation time (7) as settings and the TW arrival time difference ( $t_s - t_r$ ) as the measurement. If so, we obtain a fault location ( $M^*$ ) as illustrated in Fig. 2. This fault location is not accurate and represents a fictitious fault ( $F^*$ ) shown in Fig. 2.

Note, however, that the TW arrival time difference ( $t_s - t_r$ ) applies to the actual fault ( $F$ ) and its true location ( $M$ ). Therefore, we simply correct the result ( $M^*$ ) by projecting it from the straight-line characteristic representing a homogeneous power line in Fig. 2, to the actual line characteristic representing the hybrid line ( $F^* \rightarrow F$  in Fig. 2b).

We summarize our double-ended TW-based fault-locating method for hybrid (nonhomogeneous) lines as follows:

Step 1. Calculate the fault location ( $M^*$ ) with (4) as if the line were homogeneous, i.e., using the total line length and the total TW line propagation time.

- Step 2. Calculate the propagation time ( $t^*$ ) corresponding to the fault location ( $M^*$ ) assuming the line is homogeneous, i.e., using the straight line between the origin and the point defined by the total line length and the total TW line propagation time.
- Step 3. Calculate the actual fault location ( $M$ ) corresponding to the propagation time ( $t^*$ ) using the nonhomogeneity distance-propagation time characteristic of the line.

### 3.4 Numerical example

Consider the hybrid 138 kV line depicted in Fig. 2a with the overhead line sections and underground cable section data given in Table 1.

Section	Type	Length (mi)	Propagation Time ( $\mu$ s)
1	Overhead	20.00	107.50
2	Cable	8.00	81.50
3	Overhead	10.00	53.75
Total	Hybrid	38.00	242.75

Table 1: Hybrid line data used in the numerical example.

We modeled this line with an electromagnetic transient program using data for a sample 138 kV overhead line and a 138 kV single-core coaxial underground cable.

#### 3.4.1 Example 1: Fault on the overhead section

An AG fault occurred on Section 1 of the overhead line, 15 mi from Terminal S. Fig. 3 shows the voltages and currents at Terminals S and R. Fig. 4 shows the terminal currents at the time of arrival of the first TWs. Fig. 5 shows the alpha aerial current referenced to Phase A at the output of the differentiator-smoother filter used to extract the current TWs from the measured currents.

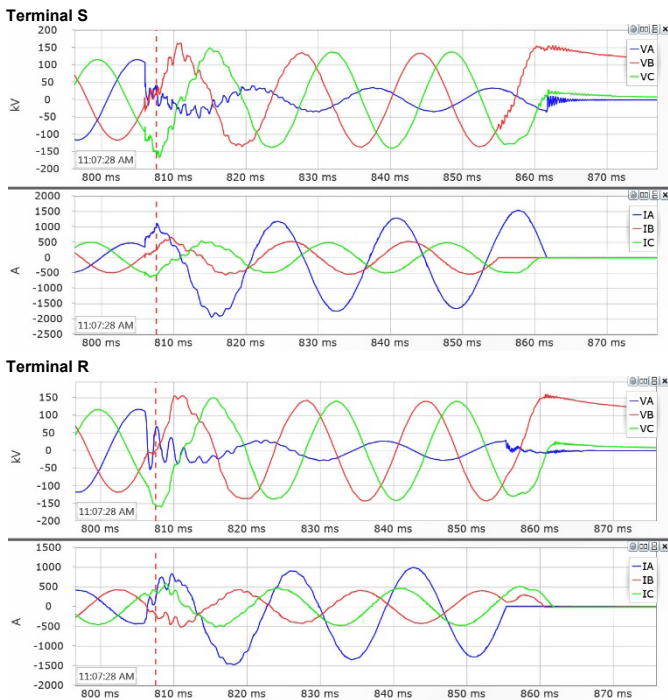


Fig. 3. Ex. 1: Voltages and currents at Terminals S and R.

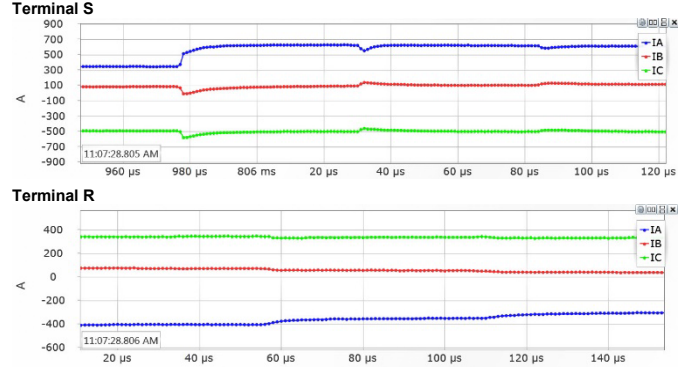


Fig. 4 Ex. 1: Currents at Terminals S and R on the time scale selected to show the first TWs arriving at the line terminals.

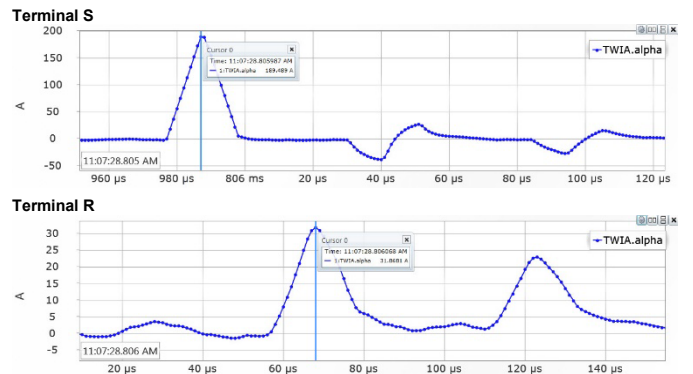


Fig. 5. Ex. 1: Very first current TWs at Terminals S and R.

The time-stamping algorithm [5] calculates the following TW arrival times at Terminals S and R for the TWs shown in Fig. 5:

$$t_s = 805,987.549 \mu\text{s} \text{ and } t_R = 806,068.341 \mu\text{s}$$

Using (4), we calculate the raw fault location as follows (Step 1):

$$M^* = \frac{38}{2} \cdot \left( 1 + \frac{5,987.549 - 6,068.341}{242.75} \right) = 12.676 \text{ mi}$$

Assuming a homogeneous line, we obtain the following TW line propagation time from Terminal S to the fault (Step 2):

$$t^* = 12.676 \cdot \frac{242.75}{38} = 80.976 \mu\text{s}$$

Using the nonhomogeneity characteristic as per Table 1, we obtain the true fault location (Step 3):

$$80.976 \mu\text{s} \rightarrow 15.066 \text{ mi}$$

The 0.066 mi error is about 350 ft (107 m), or about one-third of a tower span.

#### 3.4.2 Example 2: Fault on the underground section

A BG fault occurred on Section 2 (underground cable), 23 mi from Terminal S or 3 mi from the transition point between Section 1 and Section 2. Fig. 6 shows the voltages and currents at Terminals S and R. Fig. 7 shows the alpha aerial current referenced to Phase B at the output of the differentiator-

smoother filter used to extract the current TWs from the measured currents.

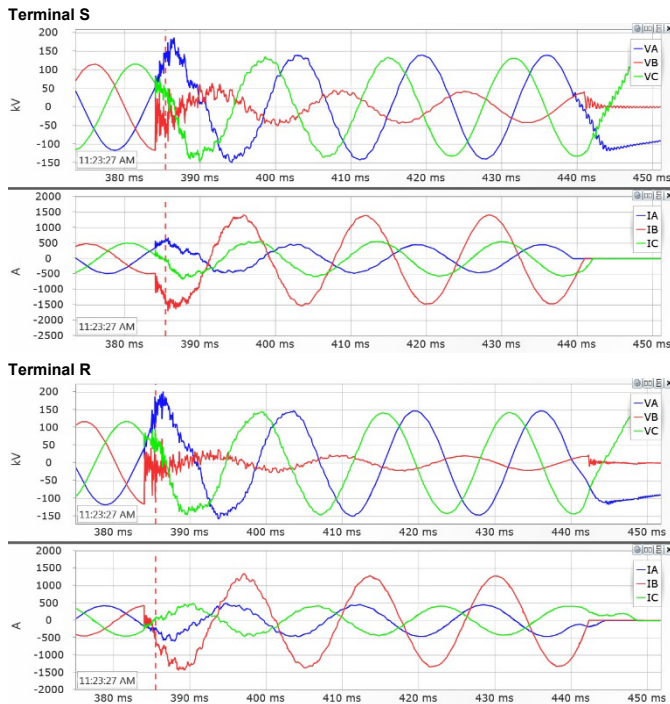


Fig. 6. Ex. 2: Voltages and currents at Terminals S and R.

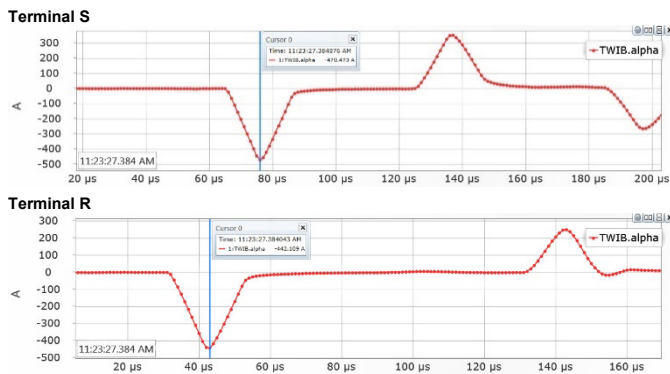


Fig. 7. Ex. 2: Very first current TWs at Terminals S and R.

The time-stamping algorithm [5] calculates the following TW arrival times at Terminals S and R for the TWs shown in Fig. 7:

$$t_s = 384,076.341 \mu\text{s} \text{ and } t_r = 384,042.813 \mu\text{s}$$

Using (4) and the three-step correction method, we obtain the fault location of 23.008 mi. The 0.008 mi error is about 42 ft (13 m).

#### 4 Adaptive autoreclosing control logic

In reference to Fig. 8, an adaptive autoreclosing logic provides settings that allow the user to specify multiple blocking regions for autoreclosing. The logic asserts an output bit a few milliseconds after the fault if the calculated fault location falls in any of the blocking regions. Apply this blocking bit as follows:

- Use this bit in your autoreclosing scheme to cancel reclosing.
- In single-pole tripping applications, use this bit to force three-pole tripping for single-line-to-ground (SLG) faults.

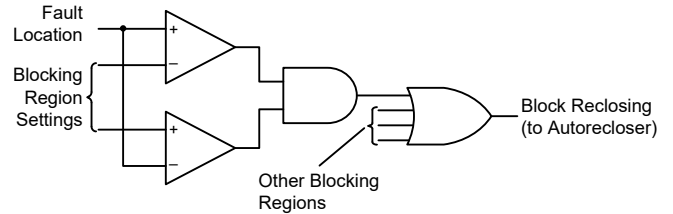


Fig. 8. Simplified autoreclosing control logic.

Apply margin when setting the blocking regions to avoid spurious reclosing onto cable faults or onto faults located in the “do not reclose” zones in other applications. Set the blocking region slightly longer than the “do not reclose” stretch of the line. Consult the manufacturer’s fault-locating accuracy specification when selecting margins.

Adaptive autoreclosing control logic may provide a setting to decide if autoreclosing shall be allowed or canceled if the fault-locating algorithm fails to locate the fault for any reason [6].

#### 5 Obtaining configuration data for better accuracy of the TW fault locator

Line length and TW line propagation time settings impact fault-locating accuracy. This section teaches how to measure the TW line (or section) propagation time to improve fault-locating accuracy.

When a power line is being energized, the closure of the circuit breaker pole applies a voltage step to the de-energized conductor, and therefore, it launches a wave that travels to the remote terminal. Because the remote circuit breaker is open, the current TW reflects completely and arrives back at the local terminal.

You can use the line energization test to measure the TW line propagation time for each section of a hybrid line. Each transition between an overhead line section and an underground cable section results in a TW reflection, i.e., a TW sent back to the energizing terminal. Fig. 9 shows an example of energizing the line of Table 1 assuming 400 A incident current TW, neglecting dispersion and attenuation, and assuming the overhead line and underground cable characteristic impedances of 300 Ω and 70 Ω, respectively. These reflections allow you to measure the TW line propagation times between the terminal and each significant discontinuity along the line in a manner similar to the time-domain reflectometry method.

Fig. 10 shows the TW signals for line energization from Terminal S with the incident TW of about 120 A (compare with Fig. 9 to understand the timing, polarity, and magnitude of the TWs reflected from the discontinuities of the line). Table 2 shows the TW arrival time results.

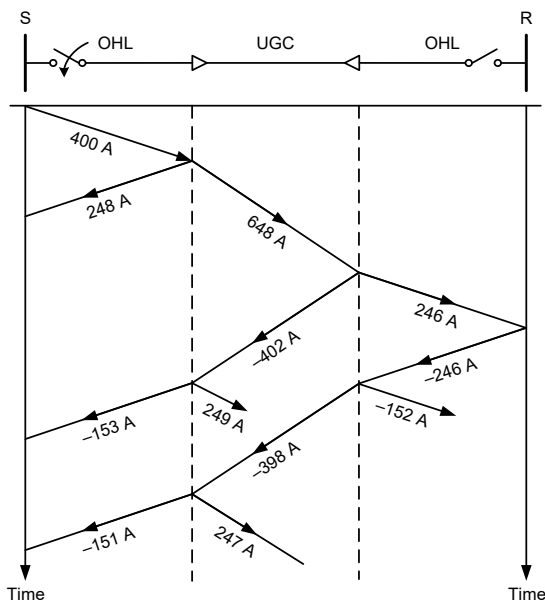


Fig. 9. Incident, reflected, and transmitted TWs for a line energization test of the hybrid line in Table 1.

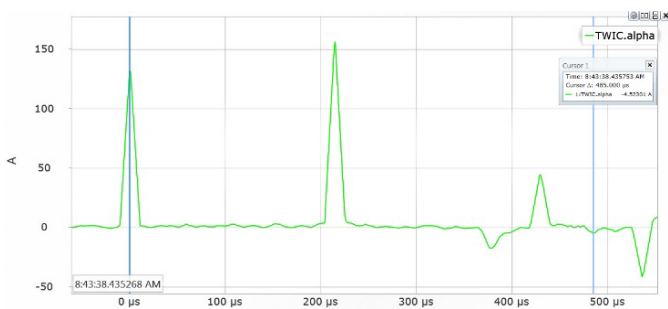


Fig. 10. Example of energizing the line in Table 1 from Terminal S. Reflections are recorded at 215, 378, and 485  $\mu$ s following the TW launched by the Phase C pole closure. The second cursor identifies the reflection arriving at 485  $\mu$ s.

Section	Round Trip	Round Trip Time ( $\mu$ s)
Energizing from Terminal S		
1	From Terminal S to the Section 1–2 transition	215.0
1+2	From Terminal S to the Section 2–3 transition	378.0
1+2+3	From Terminal S to Terminal R	485.0

Table 2: Propagation times measured during line energization.

Based on energization from Terminal S, we obtain these section TW propagation times:

- Section 1:  $0.5 \cdot 215 \mu\text{s} = 107.5 \mu\text{s}$
- Section 2:  $0.5 \cdot (378 - 215) \mu\text{s} = 81.5 \mu\text{s}$
- Section 3:  $0.5 \cdot (485 - 378) \mu\text{s} = 53.5 \mu\text{s}$

Note that the differences between the line energization results and the propagation times in Table 1 are very small, around a quarter of a microsecond.

## 6 Conclusions

In this paper, we discussed the benefits of using fault location to adaptively control autoreclosing for power lines—to allow reclosing for some fault locations and to prevent reclosing for other fault locations along the line. These applications include blocking autoreclosing for faults on underground cable sections of hybrid lines, line sections in fire-prone rural terrains, near small airports, or in urban areas.

This paper explains how to extend the original double-ended TW-based fault-locating method derived for homogeneous lines, to hybrid lines in which the cable and overhead sections have different TW propagation velocities. The method is simple to implement and apply. It requires time synchronization and communications, but only between the main terminals of the line and not between the terminals and each overhead-to-cable transition point. It has accuracy on the order of 300 m (1000 ft) for faults on overhead line sections, and 150 m (500 ft) for faults on cable sections.

The paper presents operation examples from the double-ended TW-based fault locator integrated with an adaptive autoreclosing control logic implemented in a relay [6].

Performing line energization tests is a recommended practice to obtain accurate settings for the TW-based fault locator and the adaptive autoreclosing control logic.

## 7 References

- [1] B. Kasztenny, A. Guzmán, M. V. Mynam, and T. Joshi, “Locating Faults Before the Breaker Opens – Adaptive Autoreclosing Based on the Location of the Fault,” proceedings of the 44th Annual Western Protective Relay Conference, Spokane, WA, October 2017.
- [2] C37.104-2002 – IEEE Guide for Automatic Reclosing of Line Circuit Breakers for AC Distribution and Transmission Lines.
- [3] P. Orr, G. Fusiek, C. D. Booth, P. Niewczas, A. Dysko, F. Kawano, P. Beaumont, and T. Nishida, “Flexible Protection Architectures Using Distributed Optical Sensors,” proceedings of the 11th IET International Conference on Developments in Power System Protection, Birmingham, UK, April 2012.
- [4] D. Tziouvaras, “Protection of High-Voltage AC Cables,” proceedings of the 32nd Annual Western Protective Relay Conference, Spokane, WA, October 2005.
- [5] E. O. Schweitzer, III, A. Guzmán, M. V. Mynam, V. Skendzic, B. Kasztenny, and S. Marx, “Locating Faults by the Traveling Waves They Launch,” proceedings of the 40th Annual Western Protective Relay Conference, Spokane, WA, October 2013.
- [6] SEL-T400L Time-Domain Line Protection Instruction Manual. Available: <https://selinc.com>.